Complexation and extraction studies of trivalent actinides and lanthanides with water-soluble and CHON compatible ligands for the selective extraction of americium

Patrik Weßling,*[a,b] Melina Maag,[b] Giana Baruth,[a,b] Thomas Sittel,[a] Fynn S. Sauerwein,[c] Andreas Wilden,[c] Giuseppe Modolo,[c] Andreas Geist,[a] and Petra J. Panak[a,b]

[a]Karlsruhe Institute of Technology (KIT), Institute for Nuclear Waste Disposal (INE), P.O. Box 3640, 76021 Karlsruhe, Germany. E-mail: patrik.wessling@partner.kit.edu; Tel: +49 (0)721 608 24652

[b]Heidelberg University, Institute of Physical Chemistry, Im Neuenheimer Feld 234, 69120 Heidelberg, Germany

[c]Forschungszentrum Jülich GmbH, Institut für Energie und Klimaforschung – Nukleare Entsorgung (IEK-6), 52428 Jülich, Germany

Abstract

Novel hydrophilic ligands to selectively separate Am(III) are synthesized: 3,3'-([2,2'-bipyridine]-6,6'-diylbis(1H-1,2,3-triazole-4,1-diyl))bis(propan-1-ol) (PrOH-BPTD) and 3,3'-([2,2'-bipyridine]-6,6'-diylbis(1H-1,2,3-triazole-4,1-diyl))bis(ethan-1-ol) (EtOH-BPTD). The complexation of An(III) and Ln(III) with PrOH- and EtOH-BPTD is studied by time-resolved laser fluorescence spectroscopy (TRLFS). $[ML_2]^{3+}$ is found for both Cm(III) and Eu(III) while $[ML]^{3+}$ is only formed with Cm(III). Stability constants show a preferential coordination of Cm(III) over Eu(III) with PrOH-BPTD being the stronger ligand. The distribution of Am(III), Cm(III) and Ln(III) between an organic phase containing the extracting agent N,N,N′,N′-tetra-n-octyl-3-oxapentanediamide (TODGA) and aqueous phases containing PrOH-BPTD is studied as a function of time and temperature as well as the TODGA, BPTD and HNO_3 concentrations. A system comprised of 0.2 mol/L TODGA and 0.04 mol/L PrOH-BPTD in 0.33 – 0.39 mol/L HNO_3 allows for selective Am(III) back-extraction into the aqueous phase while keeping Cm(III) and Ln(III) in the organic phase marking PrOH-BPTD as an excellent complexant for an optimized AmSel process (Am(III) Selective Extraction).

Introduction

Many countries are trying to innovate their nuclear fuel cycle in order to reduce the long-term radiotoxicity and the long-term heat load of their nuclear waste. One major strategy is the separation of the transuranium elements (TRU) and their subsequent recycling as nuclear fuel.[1-2] Therefore, the development of new pyro- and hydrometallurgical separation processes is underway in many countries to separate the TRU from irradiated nuclear fuel. Many endeavors focus on hydrometallurgical separation processes, where a target solute is extracted from an aqueous phase into an organic phase containing a lipophilic extracting agent, separating it from other solutes. The target solute is then back-extracted (stripped) into a different aqueous phase, allowing its further processing, while the organic phase is re-used for further extraction. Such processes can be combined with an advanced PUREX process that separates uranium, plutonium and neptunium from spent nuclear fuel.[3] Over the years numerous extraction processes[4] have been developed to separate both Am(III) and Cm(III) from the advanced PUREX raffinate in one process (e.g. 1c-SANEX[5-6], i-SANEX[6-9], ALSEP[10]) or in a combination of two processes (DIAMEX + SANEX).[11-16] The final result of these processes or combination of such is an aqueous solution containing Am(III) and Cm(III) intended for further fuel fabrication. Since all curium isotopes in spent nuclear fuel are short-lived handling of new fuels and their fabrication is most complex due to the high neutron dose rates, activities and the resulting heat load. Consequently, extraction processes that aim at exclusively

separating Am(III) from PUREX raffinate have been developed. These processes have to master the separation of Am(III) and Cm(III) which is extremely difficult due to their almost identical ionic radii[17] and them both being An(III). This challenging task has been tackled by oxidation[18-21] of Am(III) (e.g. SESAME[22-24]) or by the use of special diluents and soft-donor extractants (e.g. LUCA, EXAm).[25-27]

One process that successfully achieves this challenging separation is the AmSel (Am(III) Selective Extraction) process:[28] An(III) and Ln(III) are coextracted from PUREX raffinate at high [HNO_3] by N,N,N′,N′-tetra-n-octyl-3-oxapentanediamide (TODGA, Scheme 1) dissolved in a mixture of kerosene and 1-octanol. Afterwards Am(III) is back-extracted from the loaded organic phase into an aqueous phase at low [HNO_3] containing the tetradentate complexant sodium 3,3',3'',3'''-([2,2'-bipyridine]-6,6'-diylbis(1,2,4-triazine-3,5,6-triyl))tetrabenzenesulfonate (SO_3-Ph-BTBP, Scheme 1). The process utilizes the inverse selectivity of both ligands ($SF_{Cm/Am}$(TODGA) = 1.6[29]; $SF_{Am/Cm}$(SO_3-Ph-BTBP) = 1.6[30]) resulting in a separation factor of $SF_{Cm/Am} \approx 2.5$.[28] Ln(III) are not back extracted by SO_3-Ph-BTBP due to its low affinity for the latter. Proper adjustment of SO_3-Ph-BTBP and HNO_3 concentrations results in Cm(III) and Ln(III) distribution ratios larger than one (keeping them largely in the organic phase) and an Am(III) distribution ratio smaller than one (allowing for its selective back-extraction).

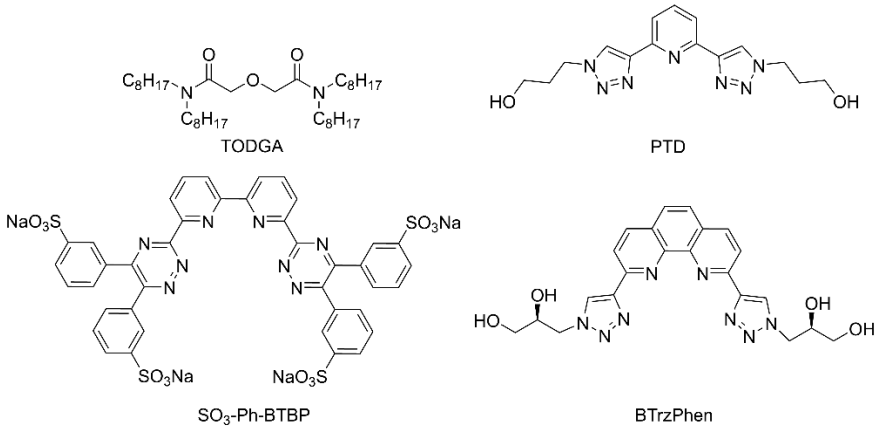

Scheme 1 Molecular structure of TODGA, SO_3-Ph-BTBP, BTrzPhen and PTD.

Nowadays, new solvents and molecules for spent nuclear fuel reprocessing should be CHON compatible meaning that new complexants and extractants are solely comprised of carbon, hydrogen, oxygen and nitrogen to avoid the generation of secondary waste and assure complete combustibility[31]. As SO_3-Ph-BTBP is not CHON compatible new water-soluble ligands are needed that fulfil the CHON requirement. A first attempt has been made by Edwards et. al. who synthesized 2,9-bis-(1H-1,2,3-triazol-4-yl)-1,10-phenanthrolines (BTrzPhen, Scheme 1). Although the TODGA/BTrzPhen system shows an Am/Cm selectivity ($SF_{Cm/Am}$ = 2.5) distribution data for light lanthanides are missing. Thus, no assessment about the selectivity between Am(III) and the light lanthanides, which is often the limiting factor for such systems, can be made[32]. Another CHON compatible and water-soluble ligand is 3,3'-(pyridine-2,6-diylbis(1H-1,2,3-triazole-4,1-diyl))bis(propan-1-ol) (PTD, Scheme 1)[8-9, 33]. PTD is able to back-extract actinides from a loaded TODGA solvent and, thus, separate them from the lanthanides. However, it does not show a selectivity between Am(III) and Cm(III).

In order to drive the development of new recycling strategies forward a new type of molecules is envisioned that combines the Am/Cm selectivity of tetradentate BTBPs[28] with the solubility of the CHON compatible PTD. The products of this combination are 6,6'-bis(1-butyl-1H-1,2,3-triazol-4-yl)-2,2'-bipyridines (BPTDs, Scheme 2).

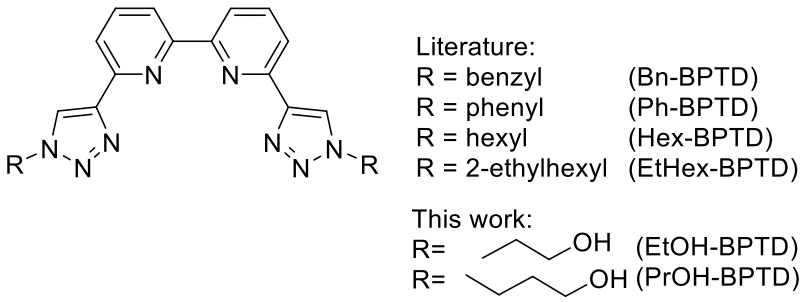

Scheme 2 Molecular structures of the literature known lipophilic BPTDs as well as the new hydrophilic BPTDs.

Lipophilic BPTDs are known from the literature [34-36]. Hex-BPTD and Ph-BPTD have been synthesized in order to form stable Ru(II) complexes in an ethanol/water mixture.[35] EtHex-BPTD has been specifically synthesized for the separation of An(III) from Ln(III). With the assistance of an anion source (2-bromohexanoic acid) *Muller et. al* demonstrated that EtHex-BPTD separates Am(III) from Eu(III) with a separation factor of 70 ($[HNO_3] \leq 0.1$ mol/L).[36] Moreover, using TRLFS it has been shown that Eu(III) is extracted into toluene as a mixture of 1:1 and 1:2 complexes.[34] Finally, a crystal structure of a 1:1 complex of Ce(III) and Bn-BPTD exists in which Ce(III) is coordinated in a tenfold manner.[34] However, so far no hydrophilic BPTD have been reported in the literature.

For this study the new hydrophilic CHON ligands 3,3'-([2,2'-bipyridine]-6,6'-diylbis(1H-1,2,3-triazole-4,1-diyl))bis(propan-1-ol) (PrOH-BPTD) and 3,3'-([2,2'-bipyridine]-6,6'-diylbis(1H-1,2,3-triazole-4,1-diyl))bis(ethan-1-ol) (EtOH-BPTD) have been synthesized (Scheme 2). In order to test the performance of PrOH- and EtOH-BPTD and to gain insight into their complexation chemistry a combined approach of solvent extraction and time-resolved laser fluorescence spectroscopy (TRLFS) is followed.

Experimental

Chemicals

Caution! ^{248}Cm, ^{244}Cm ^{241}Am, ^{154}Eu and ^{152}Eu are α-, β^--, β^+- and/or γ-emitters. They have to be handled in dedicated facilities with appropriate equipment for radioactive materials to avoid health risks caused by radiation exposure.

PrOH-BPTD and EtOH-BPTD were synthesized as described below (cf. Synthesis). Deuterated solvents were purchased from Deutero GmbH. All commercially available chemicals and solvents were bought from Merck, Alfa Aesar, TCI chemicals or Technocomm and used without further purification.

Solvent extraction

Organic phases were 0.05 – 0.3 mol/L N,N,N′,N′-tetra-n-octyl-3-oxapentanediamide (TODGA)[29, 37-39] in kerosene (TPH) containing 5 Vol.% of 1-octanol. Aqueous phases contained 0.01 – 0.05 mol/L PrOH- or EtOH-BPTD in HNO_3. Aqueous phases were spiked with 1 kBq/mL of ^{241}Am(III) and ^{154}Eu(III) (in some cases ^{152}Eu(III) instead of ^{154}Eu(III)). If necessary 1 kBq/mL of ^{244}Cm(III) and 6 mg/mL $Ln(NO_3)_3$ (La, Ce-Lu w/o Pm) were added.

Each 500 µL of aqueous and organic phase were placed in a 2 mL screw cap vial and shaken for 30 min at 298 K on an orbital vortex shaker (2500 rpm). This time proved sufficient to reach the chemical equilibrium. After centrifugation (2 min) 300 µL of each phase were separated.

Activities of ^{241}Am, ^{154}Eu and ^{152}Eu were measured using γ-counting (Packard Cobra Auto-Gamma 5003). Activities of ^{244}Cm and ^{241}Am were determined by α-spectrometry after stripping of the organic phases into 0.5 mol/L

ammonium glycolate solution (pH = 4, A/O = 10) and diluting aqueous phases with the same solution. Concentrations of inactive metal ions were determined by ICP-MS after dilution with 2 % ultrapure HNO_3.

TRLFS sample preparation

4.7 µL of a $2.12 \cdot 10^{-5}$ mol/L $Cm(ClO_4)_3$ in 0.01 mol/L $HClO_4$ were added to 995.3 µL of 10^{-3} mol/L $HClO_4$, 0.5 mol/L $HClO_4$ or 0.5 mol/L HNO_3 resulting in an initial Cm(III) concentration of 10^{-7} mol/L. In case of Eu(III) 9.4 µL of a $1.07 \cdot 10^{-3}$ mol/L $Eu(ClO_4)_3$ solution in 0.01 mol/L $HClO_4$ was added to 990.6 µL of 10^{-3} mol/L $HClO_4$ or 0.5 mol/L $HClO_4$. For Eu(III) experiments in 0.5 mol/L HNO_3 nitrate solutions and HNO_3 with the respective concentrations were used.

Stock solutions of PrOH- and EtOH-BPTD in 10^{-3} mol/L $HClO_4$, 0.5 mol/L $HClO_4$ and 0.5 mol/L HNO_3 were prepared. If needed dilutions were prepared maintaining the solvent matrix. The ligand concentration was adjusted by adding appropriate volumes of ligand solution. TRLFS spectra were recorded after an equilibration time of 10 min. Prior studies proved this time sufficient to attain chemical equilibrium.

Solvent extraction samples for TRLFS measurements were prepared as described in Solvent Extraction, with the exception that the aqueous phase was spiked with 4.7 µL of the Cm(III) or 9.4 µL of Eu(III) stock solution instead of ^{241}Am and ^{154}Eu.

TRLFS measurements

TRLFS experiments were performed at 298 K with a Nd:YAG (Surelite II laser, Continuum) pumped dye laser system (NarrowScan D-R; Radiant Dyes Laser Accessories GmbH; used dye: Exalite 398 dissolved in 1,4-dioxane). A wavelength of 394.0 nm (Eu(III)) or 396.6 nm (Cm(III)) was used to excite the metal ions. Spectral decomposition was performed with a spectrograph (Shamrock 303i, ANDOR) with 1199 lines per mm gratings. The fluorescence was detected by an ICCD Camera (iStar Gen III, ANDOR). A delay of 10 µs was used to discriminate short-lived organic fluorescence and light scattering.

NMR measurements

NMR spectra were recorded on a Bruker Avance III 400 spectrometer operating at 400.13 MHz for ^{1}H, 100.63 MHz for ^{13}C and 40.58 MHz for ^{15}N at 300 K. The spectrometer was equipped with a broadband observe probe (BBFOplus) with direct x-magnetization detection for proton and heteronuclear detection experiments. Chemical shifts are referenced internally to TMS (δ(TMS) = 0 ppm) for ^{1}H and ^{13}C and to $^{15}NH_4Cl$ with δ($^{15}NH_4Cl$) = 0 ppm for ^{15}N. For all spectra, standard Bruker pulse sequences were used. 1D spectra of ^{1}H and ^{13}C were recorded with 32k data points and are zero filled to 64k data points. ^{15}N data at natural abundance were obtained from high resolution ^{1}H,^{15}N-HMQC spectra with a resolution of 4k data points in the indirect dimension. Signal multiplicity was determined as s (singlet), d (doublet), t (triplet), q (quartet), quint (quintet), sex (sextet), sept (septet), m (multiplet) and br. s (broad signal).

Results and discussion

Synthesis

The synthetic procedure shown in **Scheme 3** is followed to produce the two new CHON compatible BPTDs.

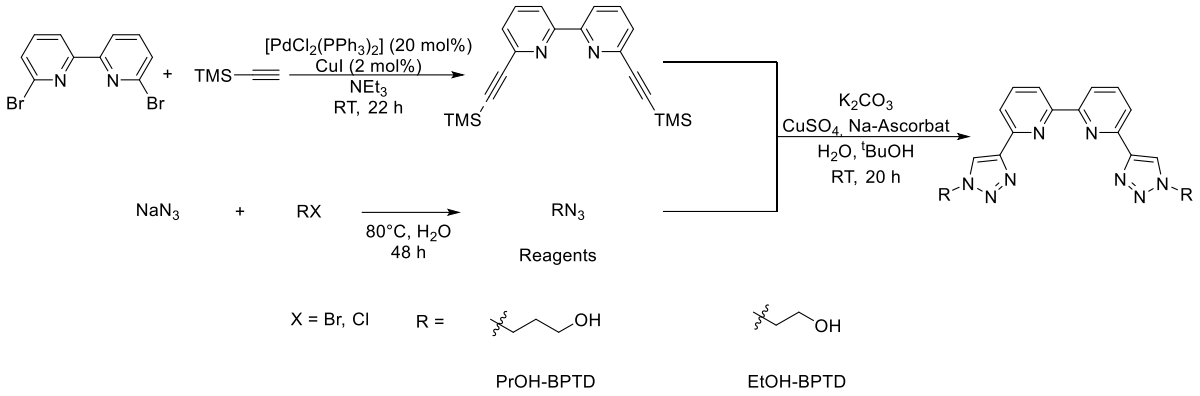

Scheme 3 Synthetic procedure of PrOH- and EtOH-BPTD.

For the synthesis of BPTDs two reagents are needed: 6,6'-Bis((trimethylsilyl)ethynyl)-2,2'-bipyridine and azido-substituted alcohols. The former is available in high yields via a literature known Sonogashira coupling.[40] The latter can be produced via nucleophilic substitution of a chloro- or bromo-alcohol-derivative with NaN_3.[9, 41] Both reagents are reacted in a copper-click reaction.[36] Following this synthetic route 2,2'-([2,2'-bipyridine]-6,6'-diylbis(1H-1,2,3-triazol-4,1-diyl))bis(propan-1-ol) (PrOH-BPTD) and 2,2'-([2,2'-bipyridine]-6,6'-diylbis(1H-1,2,3-triazol-4,1-diyl))bis(ethan-1-ol) (EtOH-BPTD) are successfully produced with a yield of 53 % and 31 %, respectively.

To increase the solubility of the new BPTDs in water short alkyl chains are chosen. However, the solubility of EtOH-BPTD is lower compared to that of PrOH-BPTD (in 2 mol/L HNO_3: PrOH: approx. 0.3 mol/L; EtOH: approx. 0.08 mol/L). Moreover, the solubility decreases with decreasing acidity (in 10^{-3} mol/L $HClO_4$: PrOH: approx. $2 \cdot 10^{-3}$ mol/L; EtOH: approx. $8 \cdot 10^{-4}$ mol/L). Although both ligands are less soluble compared to other water-soluble ligands (PTD[9]: approx. 0.15 mol/L in H_2O or dilute acid; SO_3-Ph-BTP: 0.5 mol/L in 0.5 mol/L HNO_3) their solubility is still sufficient for an application in a process for selective Am(III) separation.

Complexation of Cm(III) and Eu(III) with PrOH-BPTD in 10^{-3} mol/L $HClO_4$

Cm(III). The complexation of Cm(III) with PrOH-BPTD is studied in 10^{-3} mol/L $HClO_4$. Normalized emission spectra resulting from the $^6D'_{7/2} \rightarrow {}^8S'_{7/2}$ transition are shown in Figure 1 as a function of the PrOH-BPTD concentration. Hereby, the maximum PrOH-BPTD concentration is limited by its solubility in 10^{-3} mol/L $HClO_4$.

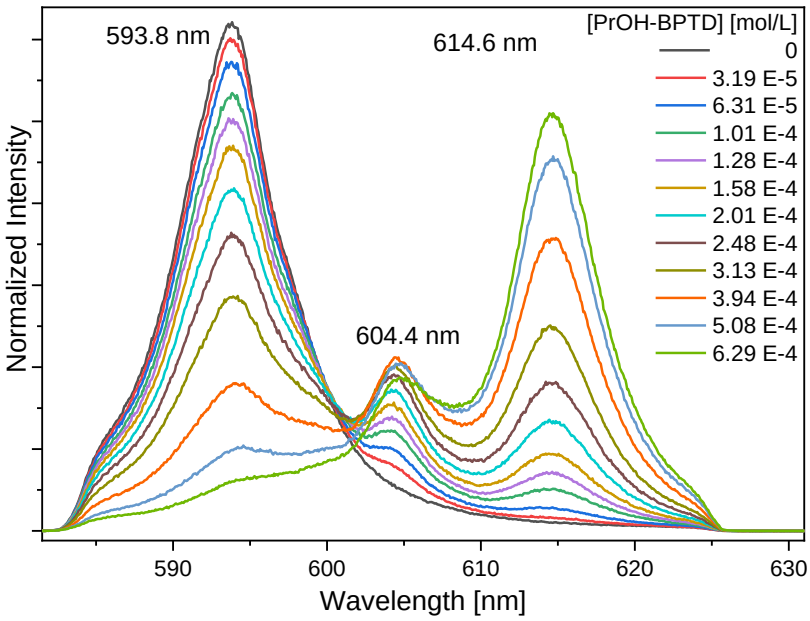

Figure 1: Normalized Cm(III) emission spectra of the complexation of Cm(III) with PrOH-BPTD in 10^{-3} mol/L $HClO_4$ as a function of the PrOH-BPTD concentration; $[Cm(III)]_{ini} = 10^{-7}$ mol/L.

In absence of PrOH-BPTD the Cm(III) aquo ion is observed (λ_{max} = 593.8 nm[42-43]). The addition of ligand leads to a bathochromic shift of the emission band to 604.4 nm and 614.6 nm. In the literature, similar shifts have been observed for other tetradentate N-donor ligands.[44-46] Therefore, the emission bands at 604.4 nm and 614.6 nm are attributed to the $[Cm(PrOH\text{-}BPTD)_n]^{3+}$ complexes (n = 1,2).

To obtain the Cm(III) speciation as a function of PrOH-BPTD peak deconvolution is employed using the relative fluorescence intensity (FI_n) factors (FI_1 = 1.0; FI_2 = 1.7, see Supporting Information (SI)). The species distribution as a function of the free ligand concentration is shown in Figure 2. The free ligand concentration is calculated according to equation (1) with $[L]_{ini}$ being the initial ligand concentration and χ_i the relative fraction of a complex species present in solution at a given ligand concentration.

$$[L]_{free} = [L]_{ini} - [Cm(III)] * (\chi_{1:1} + 2 * \chi_{1:2}) (1)$$

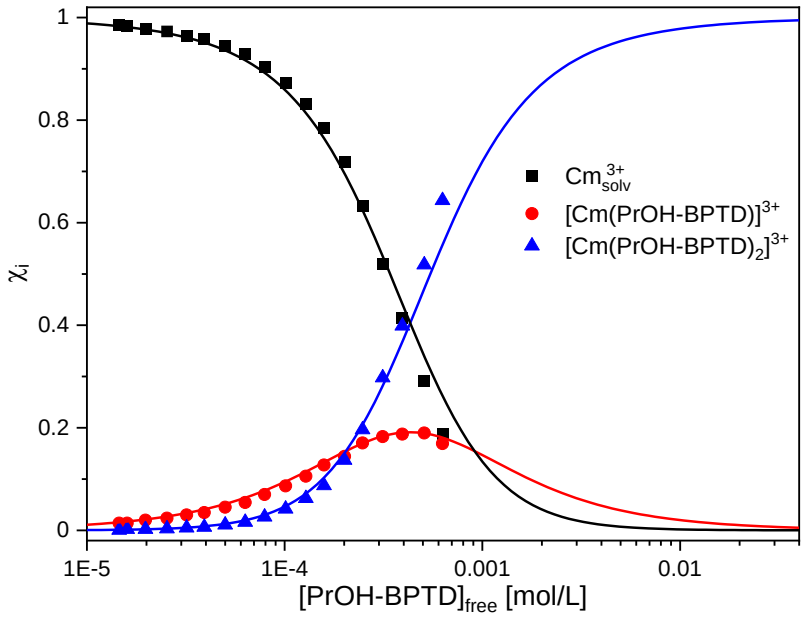

Figure 2: Fractions of $[Cm(solv.)]^{3+}$ and the $[Cm(PrOH\text{-}BPTD)_n]^{3+}$ complexes (n = 1,2) as a function the free PrOH-BPTD concentration in 10^{-3} mol/L $HClO_4$. Symbols, experimental data. Lines, calculated with log β'_1 = 3.0 and log β'_2 = 6.7.

The complexation of Cm(III) with PrOH-BPTD is observed at ligand concentrations greater 10^{-5} mol/L. The 1:1 complex reaches a maximum ratio of 19 % at $4.5 \cdot 10^{-4}$ mol/L PrOH-BPTD while for greater PrOH-BPTD concentrations the 1:2 complex becomes the dominant species.

To verify the complexation of Cm(III) with PrOH-BPTD according to a consecutive (eqn (2)) or cumulative (eqn (3)) complexation model and to confirm the assumed stoichiometries of the Cm(III)-PrOH-BPTD complexes slope analyses according to equation (4) or (5) are employed.

$$[ML_{n-1}]^{3+} + L \rightleftharpoons [ML_n]^{3+} \quad (2)$$

$$[\mathrm{M}_{Solv.}]^{3+} + \mathrm{n} * L \rightleftharpoons [ML_n]^{3+} \quad (3)$$

$$log\,\frac{c([ML_n]^{3+})}{c([ML_{n-1}]^{3+})} = 1 * log\; c\left(L_{free}\right) + log K'_n \quad (4)$$

$$log\,\frac{c([ML_n]^{3+})}{c([\mathrm{M}_{Solv.}]^{3+})} = n * log\; c\left(L_{free}\right) + log\beta'_n \quad (5)$$

Plotting log(c($[ML_n]^{3+}$)/c($[ML_{n-1}]^{3+}$)) vs. log(c(L)) results in slopes of m_1 = 1.14 ± 0.06 and m_2 = 1.12 ± 0.06 (see SI), confirming the stepwise addition of one PrOH-BPTD molecule to form 1:1 and 1:2 complexes with Cm(III).

The conditional stability constants of log β'_1 = 3.0 ± 0.1 and log β'_2 = 6.7 ± 0.3 are calculated according to eqn (6).

$$\log \beta'_n = \log\left(\frac{c([ML_n]^{3+})}{c([\mathrm{M}_{Solv.}]^{3+})\left(\mathrm{c}\left(\mathrm{L}_{free}\right)\right)^n}\right) \quad (6)$$

Eu(III). The new CHON compatible ligands need to be able to selectively strip An(III) from a loaded organic phase while the Ln(III) remain in the organic phase. Therefore, the complexation properties of PrOH-BPTD towards Ln(III) is also highly important for establishing a new extraction process. Thus, the complexation of Eu(III) with PrOH-BPTD is studied under the same conditions as for Cm(III). Hereby, Eu(III) acts as a representative for all other Ln(III) and is chosen due to its suitable fluorescence properties.

Normalized Eu(III) emission spectra of the $^5D_0 \rightarrow {}^7F_n$ transitions (n = 1,2) in 10^{-3} mol/L $HClO_4$ as a function of the ligand concentration are shown in Figure 3, left.

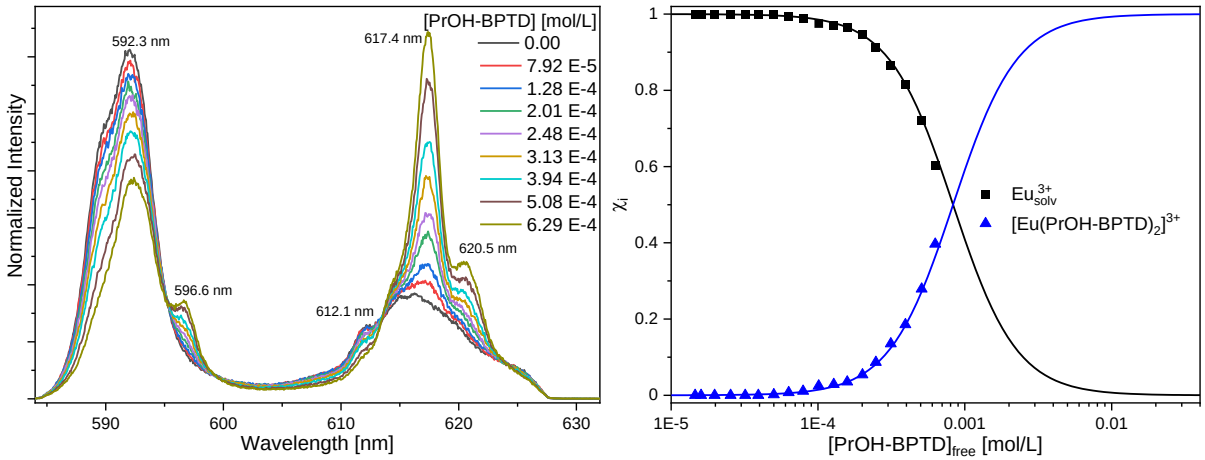

Figure 3 Left: Normalized Eu(III) emission spectra of the complexation of Eu(III) with PrOH-BPTD in 10^{-3} mol/L $HClO_4$ as a function of the PrOH-BPTD concentration; $[Eu(III)]_{ini} = 10^{-5}$ mol/L. Right: Fractions of $[Eu(Solv.)]^{3+}$ and the $[Eu(PrOH\text{-}BPTD)_2]^{3+}$ complex as function of the free PrOH-BPTD concentration in 10^{-3} mol/L $HClO_4$. Symbols, experimental data. Lines calculated with log $\beta'_2 = 6.2$.

In absence of PrOH-BPTD the spectrum of the Eu(III) aquo ion is observed with its characteristic intense $^7F_1$ emission band at 592.3 nm and a twice split and weak $^7F_2$ emission band at 612.1 nm and 616.0 nm.[47-48] Upon addition of PrOH-BPTD the intensity ratio of the $^7F_1$ and $^7F_2$ band changes which is indicative of the complexation of Eu(III) with PrOH-BPTD. The splitting of both emission bands increases with increasing ligand concentration and new emission bands at 596.6 nm, 617.4 nm and 620.5 nm are observed. The evolution of the Eu(III) emission spectra indicate the presence of only one complex species. Due to the pronounced splitting of the $^7F_2$ emission band and similarity with the 1:2 complex of Eu(III) with EtHex-BPTD[34] (cf. Scheme 2) the new species is assumed to be the 1:2 complex.

Peak deconvolution was employed to determine the speciation of Eu(III) with PrOH-BPTD in the same manner than for Cm(III) using the single component spectra shown in the SI and taking into account the following FI factor: $FI_2 = 2.8$ (see SI, for a more detailed description of peak deconvolution see references[49-50]). The speciation is shown in Figure 3, right. The complexation of Eu(III) starts at ligand concentrations greater 10^{-4} mol/L, which is almost one order of magnitude higher than for Cm(III) indicating a significantly weaker complexation of Eu(III). This is also reflected in the stability constant log $\beta'_2 = 6.2 \pm 0.4$. Moreover, slope analysis (see SI) results in a slope of $m = 2.07 \pm 0.08$, confirming the formation of the 1:2 complex.

Complexation of Cm(III) and Eu(III) with EtOH-BPTD in 10^{-3} mol/L $HClO_4$

The complexation of Cm(III) and Eu(III) with EtOH-BPTD is studied in 10^{-3} mol/L $HClO_4$ analogously to PrOH-BPTD. The normalized Cm(III) and Eu(III) emission spectra in 10^{-3} mol/L $HClO_4$ as a function of the EtOH-BPTD concentration are shown in Figure 4.

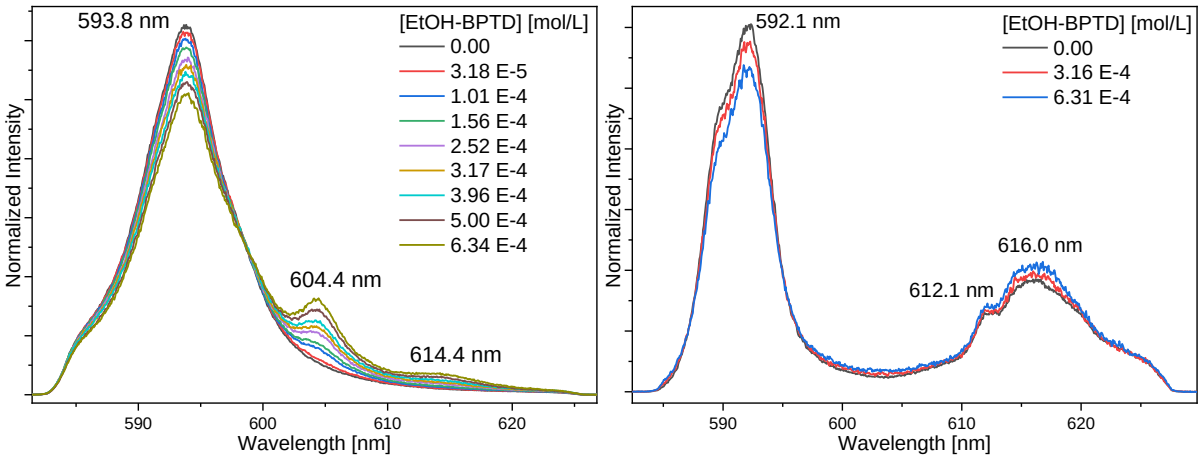

Figure 4 Normalized Cm(III) (left) and Eu(III) (right) emission spectra of the complexation of Cm(III) or Eu(III) with EtOH-BPTD in 10^{-3} mol/L $HClO_4$ as a function of the EtOH-BPTD concentration; $[Cm(III)]_{ini} = 10^{-7}$ mol/L; $[Eu(III)]_{ini} = 10^{-5}$ mol/L.

On the left side emission spectra of Cm(III) are depicted. Again, emission bands of the Cm(III) aquo ion and of the complexed species at 604.4 nm and 614.4 nm are observed although the latter is only weak in intensity even at the highest ligand concentration which is limited by the solubility of EtOH-BPTD in 10^{-3} mol/L $HClO_4$. Since EtOH- and PrOH-BPTD possess the same complexing moieties producing similar shifts in the Cm(III) emission spectra, the new emission bands are attributed to the $[Cm(EtOH\text{-}BPTD)_n]^{3+}$ complexes (n =1,2).

In Figure 4, right the emission spectra of Eu(III) are shown. In contrast to Cm(III) only minuscule changes in the emission spectrum of Eu(III) are observed upon addition of the ligand. Thus, peak deconvolution is only employed for the Cm(III) emission spectra. Slope analyses confirm the stoichiometry of the Cm(III)-EtOH-BPTD 1:1 and 1:2 complexes. Stability constants of $\log \beta'_1 = 2.6 \pm 0.1$ and $\log \beta'_2 = 4.1 \pm 0.5$ are derived for the complexation of Cm(III) with EtOH-BPTD. The $\log \beta'_2$ value of EtOH-BPTD is 2.5 orders of magnitude lower compared to that of PrOH-BPTD, providing evidence that EtOH-BPTD is a much weaker ligand compared to PrOH-BPTD under the same studied conditions. Due to its inferior complexation properties no further TRLFS and extraction studies are performed with EtOH-BPTD.

Comparison of the stability constants

To get a better understanding of the complexation properties of PrOH-BPTD in different media and to mimic conditions potentially suitable for an optimized AmSel process further TRLFS studies with PrOH-BPTD in 0.5 mol/L $HClO_4$ and 0.5 mol/L HNO_3 are performed (see SI). The stability constants for the complexation of Cm(III) and Eu(III) with PrOH- and EtOH-BPTD are summarized and compared to those of SO_3-Ph-BTBP in Table 1.

Table 1 Conditional stability constants $\log \beta'_n$ of the complexation of Cm(III) and Eu(III) with PrOH- and EtOH-BPTD as well as SO_3-Ph-BTBP in 10^{-3} mol/L, 0.5 mol/L $HClO_4$ and 0.5 mol/L HNO_3. n.d: not determined.

		10^{-3} mol/L $HClO_4$		0.5 mol/L $HClO_4$		0.5 mol/L HNO_3	
Ligand	n	Cm(III)	Eu(III)	Cm(III)	Eu(III)	Cm(III)	Eu(III)
PrOH-BPTD	1	3.0 ± 0.1	-	2.5 ± 0.2	-	2.4 ± 0.2	-
	2	6.7 ± 0.2	6.2 ± 0.4	5.0 ± 0.5	3.8 ± 0.8	4.8 ± 0.6	4.3 ± 0.4
EtOH-BPTD	1	2.6 ± 0.1	-	n.d	n.d	n.d	n.d
	2	4.1 ± 0.5	-				
SO_3-Ph-BTBP[46]	1	5.3 ± 0.2	4.9 ± 0.3	-	n.d	-	1.8 ± 0.4
	2	10.4 ± 0.4	8.4 ± 0.4	8.5 ± 0.4		7.3 ± 0.3	5.4 ± 0.5

Comparing the conditional stability constants of Cm(III) and Eu(III) with PrOH-BPTD a clear influence of the proton concentration is observed. Also, stability constants log β'_1 are less affected than log β'_2 values which decrease by almost two orders of magnitude (10^{-3} mol/L $HClO_4$ vs. 0.5 mol/L $HClO_4$). In case of hydrophilic ligands these trends are directly related to their pK_a value and the decrease in free ligand concentration under more acidic conditions which has been shown for similar ligands (e.g. SO_3-Ph-BTBP)[33, 46, 50].

Moreover, the influence of nitrate is studied as nitrate forms weak complexes with Cm(III).[51] The conditional stability constants are similar within the given error margins and, thus, no influence of nitrate on the complexation of Cm(III) or Eu(III) with PrOH-BPTD is observed.

By comparing the conditional stability constants of Cm(III) and Eu(III) a preferential complexation of Cm(III) is observed as stability constants of Eu(III) are lower by half an order of magnitude at all conditions studied. Compared to SO_3-Ph-BTBP[46] log β'_2 values of PrOH-BPTD are 2.5 – 3.7 orders of magnitude lower for Cm(III) and 1.1 - 2.2 order of magnitudes lower for Eu(III) depending on the medium. The selectivity between An(III) and Ln(III) is, also, diminished in case of PrOH-BPTD showing a trend in stability constants and selectivity between An(III) and Ln(III) if the heterocycles are changed from 1,2,4-triazines to 1,2,3-triazoles.

As already stated above EtOH-BPTD is a weaker ligand than PrOH-BPTD. This is a rather surprising observation as both ligands share the same complexing moiety and a less pronounced difference between both ligands was expected. A possible explanation could be a higher pK_a value of EtOH-BPTD in comparison to PrOH-BPTD leading to lower conditional stability constants as long as the pH value of the system is below the pK_a value of the studied ligand.

Determination of thermodynamic data for M(III)-PrOH-BPTD complex formation

For a fundamental understanding of the complexation mechanism of a metal ion with a ligand, thermodynamic data (e.g. reaction enthalpy, reaction entropy) are required. Therefore, Cm(III) (Figure 5) and Eu(III) emission spectra (see SI) at a constant ligand concentration are recorded as a function of temperature.

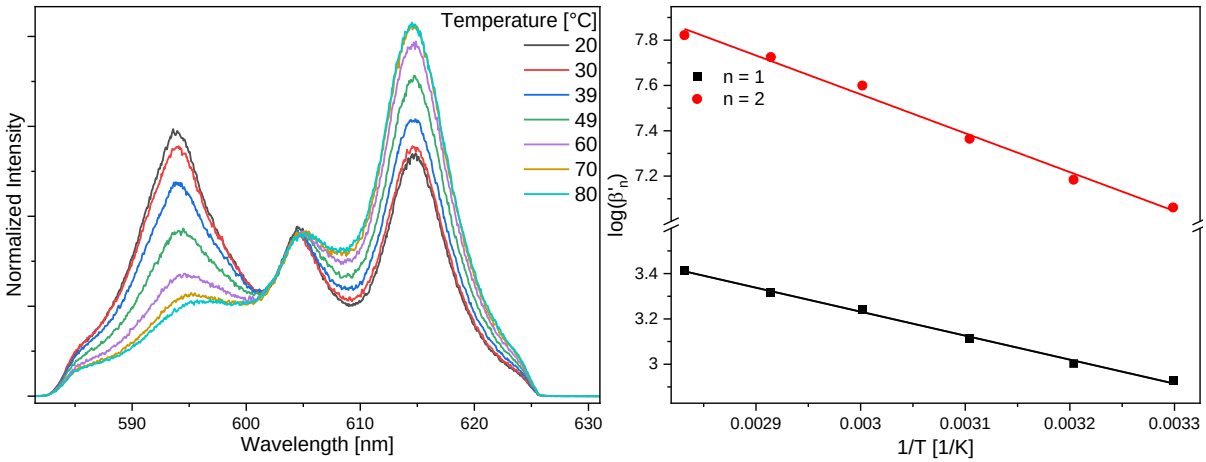

Figure 5 Left: Normalized Cm(III) emission spectra of the complexation of Cm(III) with PrOH-BPTD in 10^{-3} mol/L $HClO_4$ as a function of temperature; [PrOH-BPTD] = $2.84 \cdot 10^{-4}$ mol/L; $[Cm(III)]_{ini} = 10^{-7}$ mol/L. Right: Plot of log β'_1 and log β'_2 as a function of the reciprocal temperature and fitting according to the integrated van't Hoff equation.

The Cm(III) emission spectra at 20°C show three emission bands attributed to the Cm(III) aquo ion and the $[Cm(PrOH\text{-}BPTD)_n]^{3+}$ complexes (n = 1,2). With increasing temperature the emission band of the Cm(III) aquo ion decreases while the relative intensity of the emission band of the 1:1 and 1:2 complex increases. This indicates endothermic complexation reactions of Cm(III) with PrOH-BPTD. The conditional stability constants log β'_n are plotted as a function of the reciprocal temperature in Figure 5, right.

It is evident from **Figure 5**, right that the conditional stability constants log β'$_n$ decrease linearly with the reciprocal temperature T. Therefore, it can be assumed that the reaction enthalpy $\Delta_r H'_n$ and entropy $\Delta_r S'_n$ of both complexation steps are constant in the studied temperature range and fitting by the integrated van't Hoff equation (eqn (7)) is valid (T_0 = 298.15 K, R being the universal gas constant).

$$\log \beta'_n(T) = \log \beta'_n(T_0) + \frac{\Delta_r H'_{n,m}(T_0)}{Rln(10)}\left(\frac{1}{T_0} + \frac{1}{T}\right) (7)$$

Reaction enthalpies $\Delta_r H'_{n,m}$ are determined from the fit of the temperature dependent data according to eqn (7) while reaction entropies $\Delta_r S'_{n,m}$ are calculated using eqn (8) which is valid for small temperature intervals ($\Delta T < 100$ K) with $\Delta_R C'_{m,p} = 0$ and $\Delta_R H'_{n,m}$ = const.

$$\Delta_r G'_{n,m} = \Delta_r H'_{n,m} - \Delta_r S'_{n,m} * T = -RTln(\beta'_n) (8)$$

The reaction enthalpies $\Delta_r H'_{n,m}$ and entropies $\Delta_r S'_{n,m}$ are summarized in Table 2. The data confirm that all observed reactions for both Cm(III) and Eu(III) are endothermic and entropy driven. This is in good agreement with thermodynamic data for other tetradentate N-donor ligands, e.g. SO_3-Ph-BTBP.[46] Also, the reaction enthalpy for the first complexation step is significantly higher than for the second one. In order to form the 1:1 complex the symmetric hydration shell of Cm(III) and Eu(III) needs to be disrupted taking up more energy than attaching another PrOH-BPTD molecule in the second complexation step. This agrees with the fact that only small amounts of 1:1 complex are formed in all studied systems (cf. **Figure 2**).

Table 2 Thermodynamic data for the formation of $[M(PrOH\text{-}BPTD)_n]^{3+}$ (M = Cm, Eu; n = 1,2) in 10^{-3} mol/L $HClO_4$ according to eqn (7) and eqn (8).

	$\Delta_r H'_{n,m}$ [kJ/mol]		$\Delta_r S'_{n,m}$ [J/(mol·K)]		log β'$_n$ (20°C), calc.		log β'$_n$ (20°C), from Tab. 1.	
	Cm(III)	Eu(III)	Cm(III)	Eu(III)	Cm(III)	Eu(III)	Cm(III)	Eu(III)
n = 1	20.5 ± 3.6	-	123 ± 14	-	2.8 ± 0.4	-	3.0 ± 0.1	-
n = 2	32.9 ± 4.5	22.7 ± 4.0	239 ± 25	197 ± 23	6.6 ± 0.8	6.2 ± 0.8	6.7 ± 0.2	6.2 ± 0.4

Extraction of Ln(III), Am(III) and Cm(III) with PrOH-BPTD

In order to establish whether PrOH-BPTD is a suitable alternative for SO_3-Ph-BTBP a broad solvent extraction study is set up to gather distribution ratios for Ln(III) and An(III) as a function of the following parameters: time (see SI), temperature, HNO_3 concentration as well as complexant and extractant concentration.

Influence of the HNO_3 concentration. First extraction experiments with ^{241}Am. ^{244}Cm, ^{152}Eu, Y(III), La(III) and all Ln(III) except Pm(III) are performed using 0.1 mol/L TODGA dissolved in TPH/1-octanol (5 Vol.%) and 0.02 mol/L complexant in the aqueous phase. Hereby, fast kinetics (t < 10 min) are observed for the extraction system (see SI). Distribution ratios of the TODGA/PrOH-BPTD system for An(III), La(III) and the light Ln(III) (Ce-Eu) as a function of the HNO_3 concentration are shown in **Figure 6**. Distribution ratios for Y(III) and the heavier Ln(III) can be found in the SI.

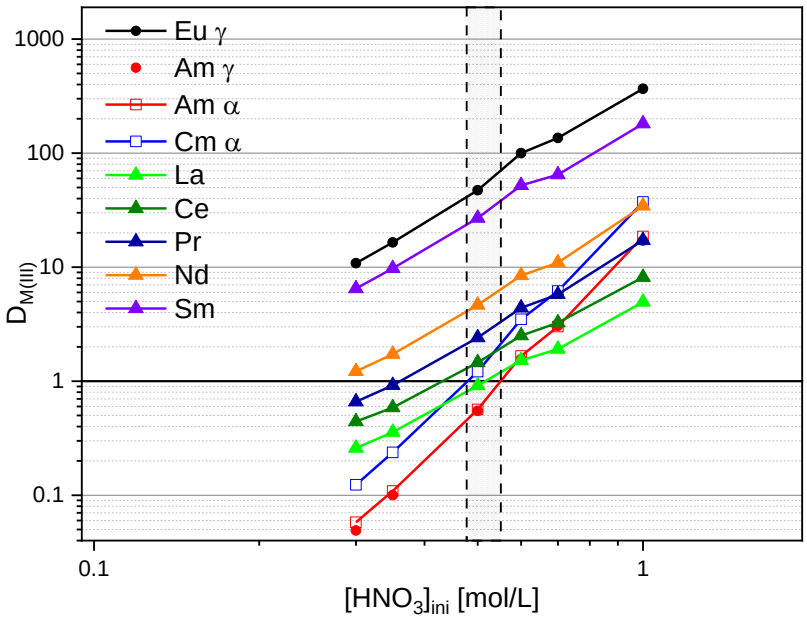

Figure 6 Distribution ratios of the extraction of ^{241}Am(III), ^{244}Cm(IIII), ^{152}Eu(III), La(III) and Ln(III) (Ce-Sm, w/o Pm) from HNO_3 solutions containing 0.02 mol/L PrOH-BPTD into 0.1 mol/L TODGA dissolved in TPH/1-octanol (5 Vol.%); T = 20°C, t = 15 min, A/O = 1. Marked section denotes the nitric acid ranges for Cm/Am separation.

The distribution ratios of all metal ions increase with increasing HNO_3 concertation, which is indicative of a solvating complexation model and in agreement with the enhanced formation of $[M(TODGA)_3](NO_3)_3$ upon increasing HNO_3 concentration. At constant HNO_3 concentrations the distribution ratios increase with decreasing ionic radii resulting in the highest distribution ratios for the heavier Ln(III).

For a viable Cm(III)/Am(III) separation D_{Am} needs to be smaller than one while D_{Cm} has to be greater than one. This is the case for 0.48 mol/L < $[HNO_3]$ < 0.55 mol/L. However, no efficient separation from La(III) is achieved in this concentration range. To increase the distribution ratios of La(III) and the light lanthanides the TODGA concentration is increased by a factor of two. As this would, however, enhance the distribution ratios of Am(III) and Cm(III) the PrOH-BPTD concentration is doubled, too, counteracting their extraction by TODGA. The distribution ratios for the optimized system are shown in Figure 7.

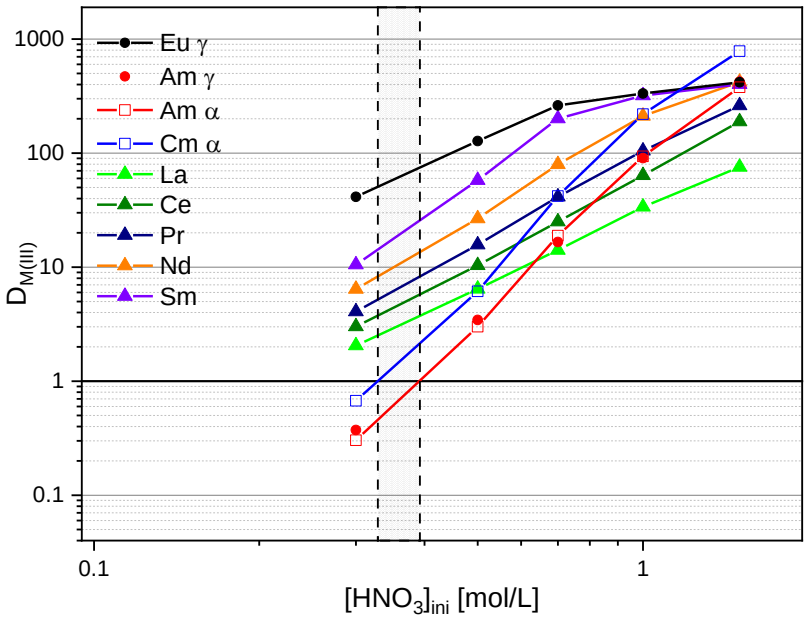

Figure 7 Distribution ratios of the extraction of ^{241}Am(III), ^{244}Cm(IIII), ^{152}Eu(III), La(III) and Ln(III) (Ce-Sm, w/o Pm) from HNO_3 solutions containing 0.04 mol/L PrOH-BPTD into 0.2 mol/L TODGA dissolved in TPH/1-octanol (5 Vol.%); T = 20°C, t = 30 min, A/O = 1. Marked section denotes the nitric acid ranges for Cm/Am separation.

As expected the distribution ratios of all metal ions increase due to the higher TODGA concentration while maintaining the selectivity of the system ($SF_{Cm/Am}$ = 2.0 – 2.3, $SF_{La/Am}$ = 6). Separation of Am(III) (D_{Am} < 1) from Cm(III) and all Ln(III) ($D_{Cm,Ln}$ ≥ 1) is achieved for 0.33 mol/L < $[HNO_3]$ < 0.39 mol/L.

The Cm/Am separation factor of PrOH-BPTD is similar to that of other tetradentate ligands like SO_3-Ph-BTBP and BTrzPhen while tridentate ligands like PTD and SO_3-Ph-BTP do not show a selectivity between Am(III) and Cm(III) which could be an indication that the ligand's denticity plays a significant role in its selectivity between the both actinides.

Influence of the TODGA concentration. The influence of the TODGA concentration on the distribution ratios of ^{241}Am(III) and ^{152}Eu(III) at constant HNO_3 and PrOH-BPTD concentrations is presented in the SI. Distribution ratios of both metal ions increase with the TODGA concentration with slopes in the range of 1.6 – 2.4 which would indicate the formation of a 1:2 complex in the organic phase. However, similar slopes have been found for the AmSel system in which the formation of a 1:3 complex was proven in the organic phase.[28] To clarify, Cm(III) and Eu(III) are extracted from 0.5 mol/L HNO_3 containing 0.02 mol/L PrOH-BPTD into 0.2 mol/L TODGA in TPH/1-octanol (5 Vol.%) and the organic phases are investigated by TRLFS (see SI). The emission spectra and fluorescence lifetime of both Cm(III) and Eu(III) agree with literature data of the $[M(TOGDA)_3]^{3+}$ complex (M = Cm, Eu)[52-53] confirming Ln(III) and An(III) to be extracted as 1:3 complexes with TODGA, also in the novel extraction system.

Influence of the PrOH-BPTD concentration and temperature dependent extraction. The influence of the PrOH-BPTD concentration was studied at a constant HNO_3 and TODGA concentration. The distribution ratios of ^{241}Am(III) and ^{152}Eu(III) as a function of the PrOH-BPTD concentration are shown in Figure 8, left. With increasing PrOH-BPTD concentration the distribution ratios of Am(III) decrease while those of Eu(III) remain constant in the studied concentration range. The latter is due to a limited interaction of Eu(III) and PrOH-BPTD, in agreement with the smaller stability constant of Eu(III) in comparison to Cm(III) (cf. Table 1).

Slope analysis of the distribution ratios of Am(III) results in slopes of -0.88 ± 0.10 indicating the formation of a 1:1 complex. A similar slope has been found for the extraction of Am(III) with SO_3-Ph-BTBP in in the current AmSel

system. However, speciation studies using TRLFS of the aqueous phases after extraction have proven the sole formation of the 1:2 complex under extraction conditions with SO_3-Ph-BTBP[28] and PrOH-BPTD (cf. next chapter).

For a complete understanding of the extraction process temperature dependent distribution ratios are needed. Therefore, ^{241}Am(III) and ^{152}Eu(III) are extracted at different temperatures while keeping the HNO_3, PrOH-BPTD and TODGA concentrations constant (**Figure 8**, right).

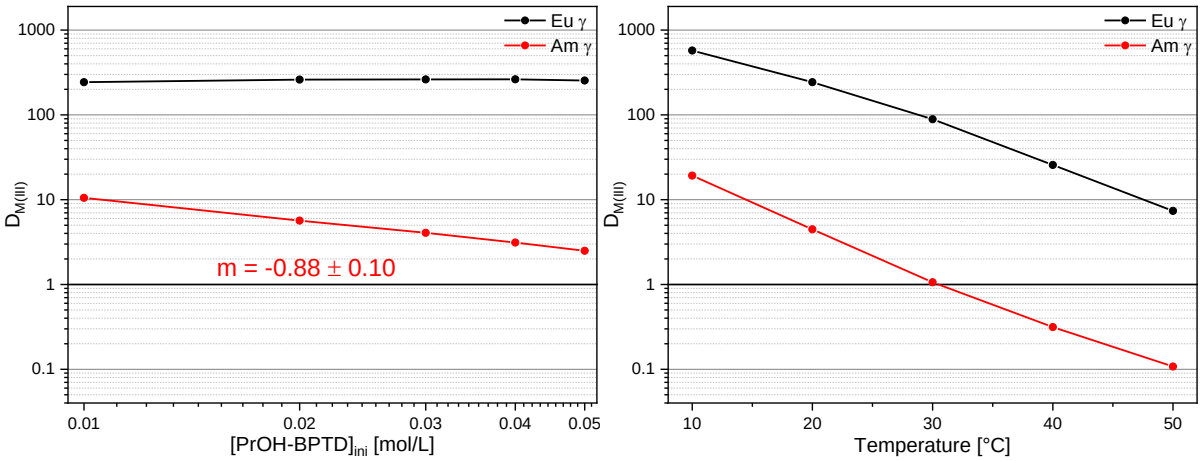

Figure 8 Distribution ratios of the extraction of ^{241}Am and ^{152}Eu from 0.5 mol/L HNO_3 into 0.2 mol/L TODGA dissolved in TPH/1-octanol (5 Vol.%) as a function of the PrOH-BPTD concentration (left) and temperature (right). Left: [PrOH-BPTD] = 0.01 – 0.05 mol/L; T = 20°C, t = 30 min, A/O = 1. Right: [PrOH-BPTD] = 0.02 mol/L; t = 30 min, A/O = 1.

The distribution ratios of both metal ions show a strong dependence on the temperature from 10°C to 50°C. Distribution ratios decrease with increasing temperature indicating an exothermic reaction. These data are of great importance as they illustrate that the HNO_3 range needed for the Cm(III)/Am(III) separation shifts to higher HNO_3 concentrations by increasing the temperature of the extraction process.

Speciation of the aqueous phase after extraction and determination of the ninth coordination site in $[Cm(PrOH\text{-}BPTD)_2]^{3+}$

In order to determine the speciation in the aqueous phase after extraction Cm(III) is extracted from HNO_3 containing PrOH-BPTD into an organic phase containing TODGA. After phase separation the aqueous phase is investigated by TRLFS. The Cm(III) emission spectrum of the aqueous phase is depicted in Figure 9 together with the single component spectra of the $[Cm(PrOH\text{-}BPTD)_2]^{3+}$ complexes in 10^{-3} mol/L $HClO_4$, 0.5 mol/L $HClO_4$ and 0.5 mol/L HNO_3.

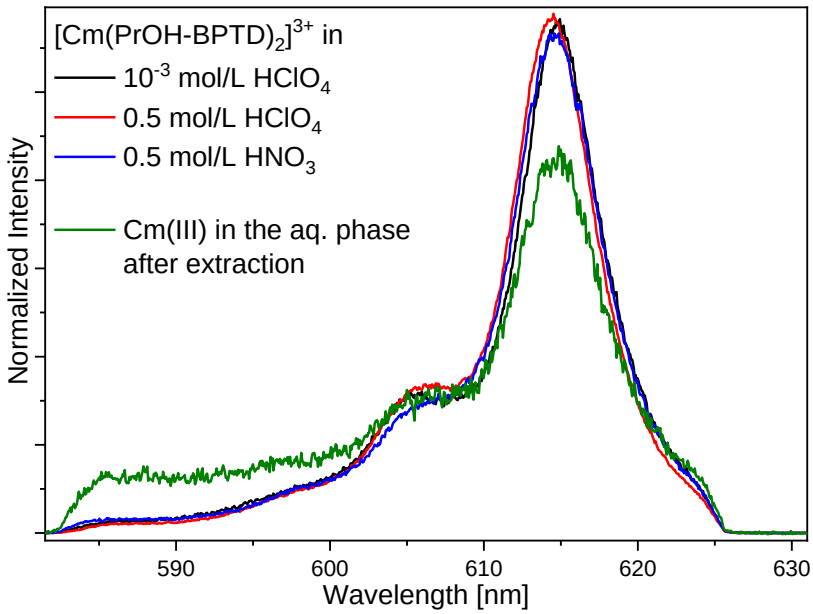

Figure 9 Normalized Cm(III) emission spectra of $[Cm(PrOH\text{-}BPTD)_2]^{3+}$ in 10^{-3} mol/L $HClO_4$, 0.5 mol/L $HClO_4$ and 0.5 mol/L HNO_3 as well as the spectrum of Cm(III) in the aqueous phase after extraction with 0.2 mol/L TODGA dissolved in TPH/1-octanol (5 Vol.%) from 0.5 mol/L HNO_3 containing 0.02 mol/L PrOH-BPTD; T = 20°C, t = 30 min, A/O = 1.

The Cm(III) emission spectrum in the aqueous phase after extraction is in excellent agreement with the single component spectra of the 1:2 complexes with PrOH-BPTD confirming Cm(III) to be present in the aqueous phase as a 1:2 complex. No evidence for the formation of a 1:1 complex is found by TRLFS. The lower signal to noise ratio of the extraction sample is due to the distribution ratio of Cm(III) which is around one.

Cm(III) is usually coordinated ninefold in solution. With PrOH-BPTD being a tetradentate ligand, one coordination site is not occupied by PrOH-BPTD in $[Cm(PrOH\text{-}BPTD)_2]^{3+}$. In the monophasic titration experiments in $HClO_4$ water occupies the ninth coordination site as the perchlorate anion is a non-coordinating anion. The comparison of $[Cm(PrOH\text{-}BPTD)_2]^{3+}$ in $HClO_4$ and HNO_3 and the aqueous phase of the extraction experiment shows that the single component spectra of the 1:2 complexes are comparable ruling out an inner-sphere coordination of nitrate. Therefore, in all cases water fills the ninth coordination site of Cm(III).

Consequently, the exact stoichiometry of the 1:2 complexes of Cm(III) with PrOH-BPTD is $[Cm(PrOH\text{-}BPTD)_2(H_2O)]^{3+}$.

Conclusions

Two novel CHON complexants for the selective stripping of Am(III) from a TODGA solvent containing Am(III), Cm(III) and Ln(III) have been synthesized with the purpose to drive the development of an optimized CHON AmSel process: 2,2'-([2,2'-bipyridine]-6,6'-diylbis(1H-1,2,3-triazol-4,1-diyl))bis(propan-1-ol) (PrOH-BPTD) and 2,2'-([2,2'-bipyridine]-6,6'-diylbis(1H-1,2,3-triazol-4,1-diyl))bis(ethan-1-ol) (EtOH-BPTD). Both ligands have been studied systematically by TRLFS and solvent extraction.

TRLFS was performed to study the complexation of Cm(III) and Eu(III) as a function of the solvent, ligand concentration and temperature. Thus, stability constants and thermodynamic data for the complexation of Cm(III) and Eu(III) in 10^{-3} mol/L $HClO_4$, 0.5 mol/L $HClO_4$ and 0.5 mol/L HNO_3 were determined. A preferential complexation of An(III) over Ln(III) was shown in all solvents with PrOH-BPTD: e.g. 10^{-3} mol/L $HClO_4$: log $\beta'_{2,Cm}$ = 6.7 vs. log $\beta'_{2,Eu}$ = 6.2. The formation of all complex species with Cm(III) and Eu(III) are endothermic and driven by entropy. Moreover, stability constants of both Cm(III) and Eu(III) decrease with increasing acidity due to an enhanced

protonation of the ligand under the studied conditions. EtOH-BPTD was found to be the inferior ligand in terms of complexation and extraction properties.

In case of PrOH-BPTD solvent extraction studies reveal fast kinetics and an exothermic extraction process. Distribution ratios of all metal ions increase with the TODGA and the HNO_3 concentration. A system comprising of 0.2 mol/L TODGA in TPH/1-octanol (5 Vol.%) and 0.04 mol/L PrOH-BPTD allows for a selective back-extraction of Am(III) ($D_{Am} < 1$) while keeping Cm and Ln(III) extracted ($D_{Cm,Ln} > 1$) in a HNO_3 concentration range of 0.33 mol/L < $[HNO_3]$ < 0.39 mol/L.

This study proves PrOH-BPTD to be an excellent and, most importantly, CHON compatible alternative for SO_3-Ph-BTBP, the complexant in the current AmSel system. The thermodynamic data and distribution ratios represent a crucial fundamental base for the development of an optimized AmSel process paving the way for CHON compatible, selective Am(III) separation.

Associated Content

SI: Synthetic procedures and NMR characterization of PrOH- and EtOH-BPTD; Single compontent spectra; evolution of the fluorescence intensity and slope analyses; Eu(III) emission spectra as a function of temperature. Distribution ratios as a function of time, for heavy Ln(III) and as a function of the TODGA concentration.

Conflicts of interest

There are no conflicts to declare.

Acknowledgements

This work has received funding from the European Research Council (ERC) under the European Union's Horizon 2020 research and innovation program (project PATRICIA, grant agreement No. 945077) and the German Federal Ministry for Research and Education (grant agreement No. 02NUK059A, 02NUK059C, 02NUK059D).

References

[1] OECD-NEA, *Advanced Nuclear Reactor Systems and Future Energy Market Needs, NEA Report No. 7566*, OECD Nuclear Energy Agency (NEA), **2021**.

[2] OECD-NEA, *Strategies and Considerations for the Back End of the Fuel Cycle, NEA Report No. 7469*, OECD Nuclear Energy Agency (NEA), **2021**.

[3] R. J. Taylor, C. R. Gregson, M. J. Carrott, C. Mason, M. J. Sarsfield, *Solvent Extr. Ion Exch.* **2013**, *31*, 442-462.

[4] A. Geist, J.-M. Adnet, S. Bourg, C. Ekberg, H. Galán, P. Guilbaud, M. Miguirditchian, G. Modolo, C. Rhodes, R. Taylor, *Separ. Sci. Technol.* **2021**, *56*, 1866-1881.

[5] A. Wilden, G. Modolo, C. Schreinemachers, F. Sadowski, S. Lange, M. Sypula, D. Magnusson, A. Geist, F. W. Lewis, L. M. Harwood, M. J. Hudson, *Solvent Extr. Ion Exch.* **2013**, *31*, 519-537.

[6] G. Modolo, A. Wilden, P. Kaufholz, D. Bosbach, A. Geist, *Prog. Nucl. Energy* **2014**, *72*, 107-114.

[7] A. Wilden, G. Modolo, P. Kaufholz, F. Sadowski, S. Lange, M. Sypula, D. Magnusson, U. Müllich, A. Geist, D. Bosbach, *Solvent Extr. Ion Exch.* **2015**, *33*, 91–108.

[8] E. Mossini, E. Macerata, A. Wilden, P. Kaufholz, G. Modolo, N. Iotti, A. Casnati, A. Geist, M. Mariani, *Solvent Extr. Ion Exch.* **2018**, *36*, 373-386.

[9] E. Macerata, E. Mossini, S. Scaravaggi, M. Mariani, A. Mele, W. Panzeri, N. Boubals, L. Berthon, M. C. Charbonnel, F. Sansone, A. Arduini, A. Casnati, *J. Am. Chem. Soc.* **2016**, *138*, 7232-7235.

[10] A. V. Gelis, G. J. Lumetta, *Ind. Eng. Chem. Res.* **2004**, *53*, 1624-1634.

[11] G. Modolo, A. Wilden, A. Geist, D. Magnusson, R. Malmbeck, *Radiochim. Acta* **2012**, *100*, 715-725.

[12] G. Modolo, A. Geist, M. Miguirditchian, (Ed.: R. J. Taylor), Woodhead Publishing, **2015**, pp. 245-287.

[13] A. Geist, U. Mullich, D. Magnusson, P. Kaden, G. Modolo, A. Wilden, T. Zevaco, *Solvent Extr. Ion Exch.* **2012**, *30*, 433-444.

[14] L. Berthon, J. M. Morel, N. Zorz, C. Nicol, H. Virelizier, C. Madic, *Separ. Sci. Technol.* **2001**, *36*, 709-728.

[15] D. Serrano-Purroy, P. Baron, B. Christiansen, R. Malmbeck, C. Sorel, J. P. Glatz, *Radiochim. Acta* **2005**, *93*, 351-355.

[16] G. Modolo, H. Vijgen, D. Serrano-Purroy, B. Christiansen, R. Malmbeck, C. Sorel, P. Baron, *Separ. Sci. Technol.* **2007**, *42*, 439-452.

[17] G. T. Seaborg, *Radiochim. Acta* **1993**, *61*, 115-122.

[18] W. H. Runde, B. J. Mincher, *Chem. Rev.* **2011**, *111*, 5723-5741.

[19] B. J. Mincher, N. C. Schmitt, M. E. Case, *Solvent Extr. Ion Exch.* **2011**, *29*, 247-259.

[20] B. J. Mincher, L. R. Martin, N. C. Schmitt, *Inorg. Chem.* **2008**, *47*, 6984-6989.

[21] Z. Wang, J.-B. Lu, X. Dong, Q. Yan, X. Feng, H.-S. Hu, S. Wang, J. Chen, J. Li, C. Xu, *J. Am. Chem. Soc.* **2022**, *144*, 6383-6389.

[22] C. Musikas, M. Germain, A. Bathellier, CEA Centre d'Etudes Nucleaires de Fontenay-aux-Roses, **1979**.

[23] G. Mason, A. Bollmeier, D. Peppard, *J. Inorg. Nucl. Chem.* **1970**, *32*, 1011-1022.

[24] L. Donnet, J. Adnet, N. Faure, P. Bros, P. Brossard, F. Josso, in *Proceedings of the 5th OECD-NEA International Information Exchange Meeting on Actinide and Fission Product Partitioning and Transmutation–Session II (Partitioning). SCK-CEN, Mol, Belgium, Nov*, Citeseer, **1998**, pp. 25-27.

[25] G. Modolo, P. Kluxen, A. Geist, *Radiochim. Acta* **2010**, *98*, 193-201.

[26] C. Rostaing, C. Poinssot, D. Warin, P. Baron, B. Lorrain, *Procedia Chem.* **2012**, *7*, 367-373.

[27] M. Miguirditchian, V. Vanel, C. Marie, V. Pacary, M.-C. Charbonnel, L. Berthon, X. Hérès, M. Montuir, C. Sorel, M.-J. Bollesteros, *Solvent Extr. Ion Exch.* **2020**, *38*, 365-387.

[28] C. Wagner, U. Müllich, A. Geist, P. J. Panak, *Solvent Extr. Ion Exch.* **2016**, *34*, 103-113.

[29] Y. Sasaki, Y. Sugo, S. Suzuki, S. Tachimori, *Solvent Extr. Ion Exch.* **2001**, *19*, 91-103.

[30] A. Geist, C. Hill, G. Modolo, M. R. S. J. Foreman, M. Weigl, K. Gompper, M. J. Hudson, C. Madic, *Solvent Extr. Ion Exch.* **2006**, *24*, 463-483.

[31] C. Madic, M. J. Hudson, *High-level liquid waste Partitioning by means of completely incinerable extractants*, EUR 18038, European Commission, Luxembourg, **1998**.

[32] A. C. Edwards, P. Mocilac, A. Geist, L. M. Harwood, C. A. Sharrad, N. A. Burton, R. C. Whitehead, M. A. Denecke, *Chemical Communications* **2017**, *53*, 5001-5004.

[33] C. Wagner, E. Mossini, E. Macerata, M. Mariani, A. Arduini, A. Casnati, A. Geist, P. J. Panak, *Inorg. Chem.* **2017**, *56*, 2135-2144.

[34] J. M. Muller, S. S. Galley, T. E. Albrecht-Schmitt, K. L. Nash, *Inorg. Chem.* **2016**, *55*, 11454-11461.

[35] J. T. Fletcher, B. J. Bumgarner, N. D. Engels, D. A. Skoglund, *Organometallics* **2008**, *27*, 5430-5433.

[36] J. M. Muller, K. L. Nash, *Solvent Extraction and Ion Exchange* **2016**, *34*, 322-333.

[37] Y. Sasaki, Y. Tsubata, Y. Kitatsuji, Y. Sugo, N. Shirasu, Y. Morita, T. Kimura, *Solv. Extr. Ion Exch.* **2013**, *31*, 401–415.

[38] S. A. Ansari, P. Pathak, P. K. Mohapatra, V. K. Manchanda, *Chem. Rev.* **2012**, *112*, 1751–1772.

[39] D. Whittaker, A. Geist, G. Modolo, R. Taylor, M. Sarsfield, A. Wilden, *Solv. Extr. Ion Exch.* **2018**, *36*, 223–256.

[40] C. Lang, K. Pahnke, C. Kiefer, A. S. Goldmann, P. W. Roesky, C. Barner-Kowollik, *Polym. Chem.* **2013**, *4*, 5456-5462.

[41] I. Domnin, L. Remizova, G. Starova, F. Rominger, *Russian journal of organic chemistry* **2009**, *45*, 1678-1682.

[42] S. Skanthakumar, M. R. Antonio, R. E. Wilson, L. Soderholm, *Inorg. Chem.* **2007**, *46*, 3485-3491.

[43] N. M. Edelstein, R. Klenze, T. Fanghanel, S. Hubert, *Coordin. Chem. Rev.* **2006**, *250*, 948-973.

[44] A. Bremer, D. M. Whittaker, C. A. Sharrad, A. Geist, P. J. Panak, *Dalton Trans.* **2014**, *43*, 2684-2694.

[45] S. Trumm, G. Lieser, M. R. Foreman, P. J. Panak, A. Geist, T. Fanghanel, *Dalton Trans.* **2010**, *39*, 923-929.

[46] C. Wagner, U. Müllich, A. Geist, P. J. Panak, *Dalton Trans.* **2015**, *44*, 17143-17151.

[47] J. L. Kropp, M. W. Windsor, *J. Chem. Phys.* **1965**, *42*, 1599-1608.

[48] J.-C. Bünzli, G. R. Choppin, *Lanthanide pobes in life, chemical and earth sciences: Theory and practice*, Elsevier Science Ltd., Amsterdam, **1989**.

[49] P. Wessling, M. Trumm, A. Geist, P. J. Panak, *Dalton Trans* **2018**, *47*, 10906-10914.

[50] P. Weßling, M. Trumm, E. Macerata, A. Ossola, E. Mossini, M. C. Gullo, A. Arduini, A. Casnati, M. Mariani, C. Adam, A. Geist, P. J. Panak, *Inorg. Chem.* **2019**, *58*, 14642-14651.

[51] A. Skerencak, J. Panak Petra, W. Hauser, V. Neck, R. Klenze, P. Lindqvist-Reis, T. Fanghänel, *Radiochim. Acta* **2009**, *97*, 385-393.

[52] A. Wilden, G. Modolo, S. Lange, F. Sadowski, B. B. Beele, A. Skerencak-Frech, P. J. Panak, M. Iqbal, W. Verboom, A. Geist, D. Bosbach, *Solvent Extr. Ion Exch.* **2014**, *32*, 119-137.

[53] P. Weßling, U. Müllich, E. Guerinoni, A. Geist, P. J. Panak, *Hydrometallurgy* **2020**, *192*, 105248.

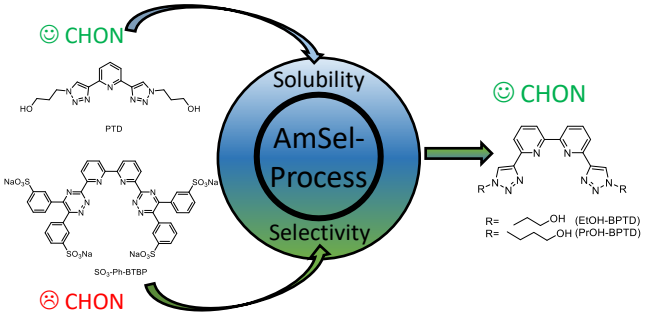

Combining the selectivity of BTBPs and the solubility of PTD, the novel ligands called “BPTDs” are synthesized for the selective extraction of americium. The complexation of Cm(III) and Eu(III) with the new ligands is studied using time-resolved laser fluorescence spectroscopy (TRLFS) and stability constants are determined. Solvent extraction is performed to assess the suitability of the new ligands for an optimized AmSel process.